Characterisation of the Predominant Low-pH Lead(II)–Hydroxo Cation, $[Pb_4(OH)_4]^{4+}$; Crystal Structure of $[Pb_4(OH)_4][NO_3]_4$ and the Implications of Basic Salt Formation on the Transport of Lead in the Aqueous Environment†

Susan M. Grimes,*[a] Simon R. Johnston[a] and Isaac Abrahams[b]

[a] *Department of Chemistry, Brunel University, Uxbridge UB8 3PH, UK*

[b] *Department of Chemistry, Queen Mary and Westfield College, University of London E1 4NS, UK*

A study of the reactions between Pb" and hydroxide ions in aqueous nitrate solutions has identified three distinct basic salt phases. When the pH is raised, the first precipitate obtained from the Pb^{2+}–NO_3^-–H_2O system is the $[Pb_4(OH)_4]^{4+}$ cluster cation. The crystal structure of $[Pb_4(OH)_4][NO_3]_4$ has been determined by single-crystal X-ray diffraction and refined by full-matrix least-squares analysis to $R_1 = 0.0706$, $wR_2 = 0.1827$. The complex crystallises in the monoclinic space group *Ia*, with $a = 18.251(5)$, $b = 17.206(5)$, $c = 18.588(12)$ Å, $\beta = 91.90(4)°$ and $Z = 16$. The Pb" atoms are contained within discrete $[Pb_4(OH)_4]^{4+}$ units. The four lead atoms are situated at the corners of a distorted tetrahedron with an average Pb–Pb distance of 3.785(4) Å and an average intracluster Pb–Pb–Pb bond angle of 60.0(1)°. The OH groups are situated above the faces of the Pb_4 tetrahedron giving each Pb atom a trigonal-pyramidal arrangement of nearest-neighbour oxygen atoms. The average Pb–OH distance is 2.38(7) Å and the average OH–Pb–OH angle 71.8(2)°. The next-nearest Pb–O distances are to nitrate O atoms with the shortest of these being in the range 2.62–2.80 Å suggesting that the non-bonding electron pairs on Pb point outwards from the cluster and cannot take part in lead–lead cluster interactions. The Raman data for the $[Pb_4(OH)_4]^{4+}$ cluster have been correlated with the crystal structure. The thermal decomposition of $[Pb_4(OH)_4][NO_3]_4$ has been studied and is rationalised in terms of a two-step dehydration of the $[Pb_4(OH)_4]^{4+}$ ion, followed by a four-step decomposition of the nitrate-containing compounds. The formation of polynuclear complexes may also depend on the total lead(II) concentration but there is no evidence from the present work for the precipitation of any phase other than $[Pb_4(OH)_4][NO_3]_4$ in the initial precipitates. Under the conditions studied, increase of the pH above 5.25, after the precipitation of $[Pb_4(OH)_4][NO_3]_4$, resulted in the replacement of NO_3^- in the lattice by OH^- and the formation of distinct phases at pH *ca.* 7 and 8.5 that are likely to be based on $[Pb_3(OH)_4]^{2+}$ and $[Pb_6O(OH)_6]^{4+}$ respectively. The implications of the formation of the Pb–OH clusters on the transport of lead in the aqueous environment have been discussed.

The speciation of lead–hydroxo moieties is important in understanding the mechanism of transport of the metal in aqueous systems. A full understanding of the environmental impact of the metal cannot be achieved without detailed knowledge of the nature of the species present in pH ranges appropriate to the aqueous environment. The characterisation of lead–hydroxo complexes in the solid state can provide a means of obtaining information on the nature of such complexes present in aqueous systems and the subsequent reactions of the precipitated materials with hydroxide ions. Several studies have been carried out on basic lead nitrate formation.[1–7] Pauley and Testerman[5] used conductometric and potentiometric titrimetry coupled with chemical analysis and solubility-product determinations to study the aqueous system $Pb(NO_3)_2$–NaOH. The resultant precipitates were found to have the empirical formulae $Pb(NO_3)_2{\cdot}Pb(OH)_2$ and $Pb(NO_3)_2{\cdot}5Pb(OH)_2$. Kwestroo *et al.*[6] prepared a range of lead-containing compounds by the addition of sodium hydroxide to a solution of lead nitrate to give known ratios of ions in the resultant solutions. The precipitates obtained were investigated by powder X-ray diffraction and chemical analysis and were said to contain four distinct products, *viz.* $Pb(NO_3)_2{\cdot}Pb(OH)_2$, $2Pb(NO_3)_2{\cdot}5Pb(OH)_2$, $Pb(NO_3)_2{\cdot}3Pb(OH)_2$ and $Pb(NO_3)_2{\cdot}5Pb(OH)_2$. Cram and Davies[8] conducted a Raman and infrared spectrophotometric study of basic lead nitrate compounds and studied their thermal decomposition products. They reported that the data for the product $Pb(NO_3)_2{\cdot}Pb(OH)_2$ were consistent with the presence of $[Pb_4(OH)_4]^{4+}$ ions.

There is evidence for the formation of two main Pb^{II}–OH clusters in lead(II) solutions over a range of pH values, *viz.* $[Pb_4(OH)_4]^{4+}$ and $[Pb_6O(OH)_6]^{4+}$. Previous studies on the formation of the $[Pb_4(OH)_4]^{4+}$ cluster in solution by electromotive force measurements[9] and X-ray scattering[10,11] indicated that the cluster contained four lead atoms situated at the corners of a tetrahedron. In a vibrational spectroscopic study of the hydrolysis of lead(II) perchlorate solutions,[12,13] analysis of the data was also consistent with the presence of $[Pb_4(OH)_4]^{4+}$ as the primary product of hydrolysis. Only one crystal structure determination of a compound containing this cluster has been reported,[14] that of $[Pb_4(OH)_4]_3[CO_3][ClO_4]_{10}{\cdot}6H_2O$, which was obtained in small amounts from hydrolysed lead(II) perchlorate solution after exposure to carbon dioxide over a period of weeks.

A larger cluster, $[Pb_6O(OH)_6]^{4+}$, has been characterised by

† *Supplementary data available:* see Instructions for Authors, *J. Chem. Soc., Dalton Trans.*, 1995, Issue 1, pp. xxv–xxx.

X-ray scattering measurements on lead(II) perchlorate solutions,[11] and by the crystal structure determinations[15,16] of two polymorphs of $[Pb_6O(OH)_6][ClO_4]_4 \cdot H_2O$.

No structural characterisations have been carried out on the nature of the first precipitate obtained when the pH of a lead(II) solution is raised. All previous structure data have been obtained from solid materials resulting from the slow hydrolysis of lead(II) perchlorate solutions. We now report on the nature of the precipitates obtained from the Pb^{2+}–OH–NO_3 system, describe the crystal structure of $[Pb_4(OH)_4][NO_3]_4$, and confirm that the first precipitate obtained is based on the $[Pb_4(OH)_4]^{4+}$ cluster ion. The Raman spectroscopic and thermoanalytical data for $[Pb_4(OH)_4][NO_3]_4$ are correlated with the structure and the implications of the nature of the lead species present on the environmental transport of lead are considered.

Experimental

A potentiometric titration of 100 cm^3 of a 0.10 mol dm^{-3} $Pb(NO_3)_2$ solution was carried out by the addition of 2 cm^3 aliquots of 0.10 mol dm^{-3} sodium hydroxide. The pH was monitored using a hydrogen-ion selective electrode. The solution was stirred constantly and a period of 3 min was allowed between each addition to achieve equilibrium. The resultant potentiometric titration curve for the pH range 2.4–11.6 is in Fig. 1. The first precipitate, formed at pH 5.25, was filtered off, washed with absolute ethanol and oven dried at 80 °C. This product, a microcrystalline powder was characterised using chemical analysis, powder X-ray diffraction and Raman and infrared spectroscopy.

Preparation of Crystalline Basic Lead(II) Nitrate.—Aliquots (1 cm^3) of an 0.1 mol dm^{-3} carbonate-free NaOH solution were added to an 0.1 mol dm^{-3} solution of $Pb(NO_3)_2$ in deionised water. The solution became turbid on the first addition of the NaOH. A period of several minutes was allowed between each addition to attain equilibrium. The changes in pH were followed using a H^+-ion selective electrode as the pH was raised from 4.20 to 5.40. At this stage the first evidence of a permanent precipitate was observed. The temperature of the solution was then raised to 60 °C, filtered into a warmed flask and seeded with previously prepared crystals. The vessel was sealed and placed in a crystallisation tank at 60 °C and the temperature lowered at a rate of 0.17 °C h^{-1} to 25 °C. At this point microcrystalline material formed. The vessel was then left sealed for several weeks until the crystals developed to a suitable size for study by single crystal X-ray diffraction. Lower quality crystals may be prepared by slow cooling of the filtered mother-liquor in an insulated flask.

Analysis.—The lead(II), nitrate and hydroxide contents of the products were determined by titration with ethylenediaminetetraacetic acid (H_4edta),[17] Nitron [Nitron = 1,4-diphenyl-3-(phenylamino)-1*H*-1,2,4-triazolium hydroxide] gravimetry,[17] and acid titration confirmed by thermal analysis, respectively. The average data Pb^{2+}, 72.0; OH^-, 6.04; and NO_3^-, 21.7% are consistent with the formulation of the basic salt as $[Pb_4(OH)_4][NO_3]_4$.

Vibrational Spectra.—The Raman spectra were recorded on a Renishaw Raman imaging microscope using the 633 nm He–Ne line for excitation. The laser power at the surface of the sample was 8mW. The scattering volume was approximately 2 μm^3 and spectra were collected from single-crystal samples between 100 and 4000 cm^{-1} with a spectral resolution of 2 cm^{-1}. The data were collected ten times with an exposure time of 23.44 s per scan. Further instrumentation details may be obtained from ref. 18. Raman spectra for a bulk-powder sample were collected in the range 200–3000 cm^{-1} using a Perkin-Elmer 1760X FT-Raman spectrometer with a liquid-nitrogen-cooled detector.

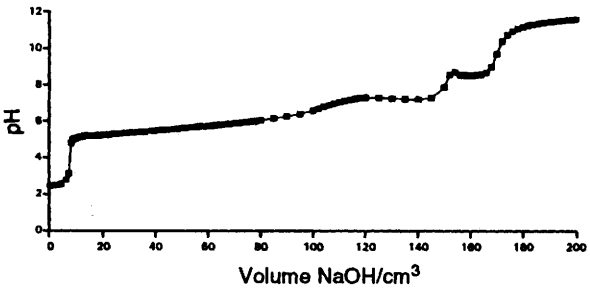

Fig. 1 Potentiometric titration of 0.10 mol dm^{-3} $Pb(NO_3)_2$ solution (100 cm^3) with 0.10 mol dm^{-3} NaOH

The spectra of the bulk-powder sample are identical to those of the single crystals used in the X-ray diffraction study. The Raman data for $[Pb_4(OH)_4][NO_3]_4$ in the range 100–2000 cm^{-1} are in Table 3.

Thermal Analysis.—Thermal decomposition data were collected on a Stanton Redcroft STA 780 thermal analyser in a flowing nitrogen atmosphere. The data were obtained at heating rates of 2, 5 and 10 °C min^{-1} from 25 to 600 °C using approximately 15 mg samples of the product in aluminium crucibles.

Crystallography.—Crystal data. $H_4N_4O_{16}Pb_4$, M = 1144.81, monoclinic, space group *Ia*, a = 18.251(5), b = 17.206(5), c = 18.588(12) Å, β = 91.90(4)°, U = 5834(4) $Å^3$, T = 298 K, D_m = 5.25 g cm^{-3}, Z = 16, D_c = 5.214 g cm^{-3}, colourless rhomboid crystals, crystal size 0.4 × 0.075 × 0.075 mm, $F(000)$ = 7808, μ(Mo-Kα) = 46.13 cm^{-1}.

Data collection and processing. Intensity data were collected on an Enraf-Nonius CAD 4 four-circle diffractometer in ω–2θ scan mode. Monochromatic Mo-Kα (λ = 0.710 69 Å) radiation was used throughout. 4377 Reflections were measured between θ 1.61 and 22.97°, of which 4194 were unique in monoclinic symmetry.

Structure analysis and refinement. Systematic absences in the intensity data indicated the possible space groups *Ia* and *I2/a* (non-standard settings of *Cc* and *C2/c*, numbers 9 and 15 respectively). The correct handedness of the space group was evaluated during the structure refinement. Attempts at a solution in the centrosymmetric group proved unsuccessful while those in the non-centrosymmetric group, *Ia*, yielded the lead atom positions by direct methods using SHELXS 86.[19] The 16 lead atoms in the asymmetric group were refined using SHELX 76[20] and used to generate the Fourier-difference map from which the oxygen and nitrogen atoms were located. The lighter atoms in the Pb-containing cluster atoms were located first and the nitrate atom positions added subsequently. Anisotropic thermal parameters were applied only to Pb atoms, and single-value average isotropic thermal parameters were used for the oxygen atoms in the Pb-containing clusters. No constraints were applied to the nitrate atoms. The hydrogen atoms were not located.

After location of all the non-hydrogen atoms, the final refinement was undertaken using SHELXL 93[21] for 3407 reflections with $I > 2\sigma(I)$. The maximum residual electron density was 6.455 e $Å^{-3}$ with an average shift/e.s.d. of 0.003. A non-unitary weighting scheme was employed in the final refinement with $w = 1/[\sigma^2(F_o^2) + (0.1000P)^2 + 0.0000P]$ where $P = (F_o^2 + 2F_c^2)/3$. Refinement was terminated with R_1 = 0.0706 and wR_2 = 0.1827 for 452 parameters. The final atomic parameters are in Table 1 and the selected contact distances and bond angles are in Table 2.

Additional material available from the Cambridge Crystallographic Data Centre comprises thermal parameters and remaining bond lengths and angles.

Table 1 Fractional atomic coordinates for $[Pb_4(OH)_4][NO_3]_4$ with estimated standard deviations (e.s.d.s) in parentheses

Atom	x	y	z	Atom	x	y	z
Pb(11)	0.9461(2)	0.9192(2)	0.1824(2)	N(90)	0.7292(37)	0.5107(38)	0.6900(36)
Pb(12)	1.0107(2)	0.9647(2)	−0.0053(2)	O(91)	0.7817(41)	0.5512(43)	0.6578(41)
Pb(13)	0.8389(2)	1.0591(2)	0.0675(2)	O(92)	0.7457(38)	0.4387(41)	0.6880(38)
Pb(14)	1.0297(2)	1.1147(2)	0.1411(2)	O(93)	0.6791(61)	0.5503(63)	0.7057(61)
Pb(21)	0.7866(2)	0.6452(2)	0.3935(2)	N(100)	0.6772(30)	0.5314(32)	0.5193(29)
Pb(22)	0.5939(2)	0.7043(2)	0.3358(2)	O(101)	0.7406(37)	0.5375(39)	0.4898(37)
Pb(23)	0.7097(2)	0.8447(2)	0.4431(2)	O(102)	0.6310(33)	0.5812(35)	0.5187(33)
Pb(24)	0.7629(2)	0.8014(2)	0.2544(2)	O(103)	0.6592(33)	0.4620(37)	0.5305(33)
Pb(31)	0.1896(2)	0.8528(2)	0.8961(2)	N(110)	0.9784(37)	0.7219(39)	0.4434(36)
Pb(32)	0.3078(2)	0.6702(2)	0.9168(2)	O(111)	0.9602(38)	0.7879(40)	0.4495(37)
Pb(33)	0.2241(2)	0.7262(2)	0.7365(2)	O(112)	0.9390(34)	0.6665(35)	0.4345(34)
Pb(34)	0.1012(2)	0.6564(2)	0.8874(2)	O(113)	1.0436(37)	0.7127(39)	0.4412(37)
Pb(41)	0.4762(2)	0.9976(2)	0.4956(2)	N(120)	0.0637(38)	0.4831(40)	0.8129(37)
Pb(42)	0.5622(2)	1.0693(2)	0.6682(2)	O(121)	0.0410(47)	0.5503(48)	0.7936(46)
Pb(43)	0.3538(2)	1.0824(2)	0.6422(2)	O(122)	0.1040(34)	0.4948(35)	0.8652(33)
Pb(44)	0.4418(2)	0.8881(2)	0.6653(2)	O(123)	0.0507(32)	0.4240(34)	0.7840(31)
O(11)	0.9096(28)	0.9741(30)	0.0559(28)	N(130)	0.4284(33)	0.7993(35)	0.2879(33)
O(12)	1.0370(29)	0.9814(30)	0.1245(29)	O(131)	0.3692(28)	0.8408(29)	0.2754(28)
O(13)	0.9641(29)	1.0834(30)	0.0300(28)	O(132)	0.4332(33)	0.7755(35)	0.3574(33)
O(14)	0.9182(29)	1.0523(30)	0.1704(29)	O(133)	0.4703(35)	0.7856(37)	0.2441(35)
O(21)	0.6805(29)	0.7046(31)	0.4313(29)	N(140)	0.8890(36)	0.4360(38)	0.3671(37)
O(22)	0.7140(29)	0.6786(30)	0.2879(29)	O(141)	0.8320(34)	0.4402(35)	0.4099(33)
O(23)	0.6657(28)	0.8170(31)	0.3221(28)	O(142)	0.9368(42)	0.4923(45)	0.3707(42)
O(24)	0.7998(29)	0.7761(29)	0.3788(29)	O(143)	0.8988(37)	0.3873(40)	0.3205(38)
O(31)	0.2822(29)	0.7814(29)	0.8459(28)	N(150)	0.2667(31)	0.5559(33)	0.2360(31)
O(32)	0.1930(29)	0.7249(29)	0.9253(28)	O(151)	0.2102(32)	0.5932(34)	0.2596(32)
O(33)	0.2190(28)	0.6346(30)	0.8243(28)	O(152)	0.2964(47)	0.5715(49)	0.1915(48)
O(34)	0.1291(29)	0.7730(29)	0.8091(28)	O(153)	0.2657(42)	0.4892(44)	0.2574(42)
O(41)	0.4639(28)	1.1029(31)	0.5812(29)	N(161)	0.5972(49)	0.5137(51)	1.3159(50)
O(42)	0.5308(29)	0.9529(31)	0.6033(29)	O(161)	0.6141(39)	0.5479(40)	1.3732(39)
O(43)	0.4476(29)	1.0182(30)	0.7083(30)	O(162)	0.5842(29)	0.5528(30)	1.2605(29)
O(44)	0.3805(29)	0.9663(30)	0.5711(29)	O(163)	0.5734(34)	0.4408(35)	1.3187(33)
N(50)	0.8230(44)	0.7476(50)	0.5622(45)	N(170)	0.8349(49)	0.5382(52)	0.8797(50)
O(51)	0.8159(26)	0.8059(27)	0.5346(26)	O(171)	0.8433(53)	0.5547(57)	0.9419(55)
O(52)	0.8100(28)	0.6770(29)	0.5323(28)	O(172)	0.7910(49)	0.5489(48)	0.8417(47)
O(53)	0.8565(39)	0.7452(43)	0.6222(40)	O(173)	0.8849(75)	0.4758(77)	0.8667(76)
N(60)	0.4370(31)	0.2802(33)	0.2669(31)	N(180)	0.1852(35)	0.5843(37)	1.0284(35)
O(61)	0.4434(33)	0.2212(35)	0.2936(32)	O(181)	0.1184(36)	0.5837(37)	1.0203(35)
O(62)	0.4934(31)	0.3132(32)	0.2390(30)	O(182)	0.2261(36)	0.5558(38)	0.9813(36)
O(63)	0.3812(26)	0.3233(29)	0.2598(27)	O(183)	0.1914(53)	0.5089(57)	1.0851(54)
N(70)	0.5174(31)	0.8022(32)	0.4818(30)	N(190)	0.0728(31)	0.7102(33)	0.6345(31)
O(71)	0.5509(35)	0.8416(37)	0.4429(36)	O(191)	0.0924(37)	0.6686(39)	0.6829(37)
O(72)	0.5278(34)	0.7326(35)	0.4939(35)	O(192)	0.1146(42)	0.7664(44)	0.6134(44)
O(73)	0.4659(28)	0.8386(29)	0.5128(28)	O(193)	0.0281(48)	0.6961(51)	0.5942(48)
N(80)	0.6407(42)	0.7104(43)	0.1339(40)	N(200)	0.8336(40)	1.2404(43)	1.0673(41)
O(81)	0.6761(32)	0.7635(36)	0.1354(33)	O(201)	0.8620(32)	1.2104(33)	1.1162(31)
O(82)	0.6421(37)	0.6552(38)	0.0896(37)	O(202)	0.8383(34)	1.2087(35)	1.0039(34)
O(83)	0.5785(34)	0.7128(35)	0.1720(34)	O(203)	0.8117(36)	1.3126(39)	1.0695(36)

Table 2 Average contact distances (Å) and bond angles (°) within a $[Pb_4(OH)_4]^{4+}$ cluster with e.s.d.s in parentheses. The maximum standard deviations for any individual Pb–Pb, Pb–O and O–O distances are 0.0063, 0.0545, and 0.0768 Å respectively, and for any individual Pb–Pb–Pb, O–Pb–O and O–O–O angles are 0.11, 2.20 and 2.00° respectively

Pb–Pb	3.785(4) (×6)	Pb–O	4.03(5) (×4)
Pb–O	2.38(7) (×12)	O–O	2.79(7) (×6)
Pb–Pb–Pb	60.0(1) (×12)	O–Pb–O	71.8(2) (×12)
Pb–O–Pb	105.5(3) (×12)	O–O–O	60.0(2) (×12)

Results and Discussion

The first precipitate obtained on the addition of hydroxide to a solution of lead(II) nitrate was identified by an X-ray diffraction study, and Raman and infrared spectroscopy as the compound $[Pb_4(OH)_4][NO_3]_4$ previously formulated as $Pb(NO_3)_2 \cdot Pb(OH)_2$.[6,8]

The crystal structure of $[Pb_4(OH)_4][NO_3]_4$ consists of isolated $[Pb_4(OH)_4]^{4+}$ clusters with nitrate ions as the counter ions. Four $[Pb_4(OH)_4]^{4+}$ units and eight nitrate groups are contained within the asymmetric unit, a projection of which is shown in Fig. 2. Fig. 3 shows the arrangement of atoms within a $[Pb_4(OH)_4]^{4+}$ cluster. The clusters consist of four lead atoms at the corners of a slightly irregular tetrahedron, with four hydroxide oxygen atoms occupying positions outside the faces of the lead tetrahedron, forming a distorted cubane structure. Each of these hydroxide oxygen atoms is co-ordinated to three lead atoms within the cluster. The average lead–lead distance is 3.785(4) Å [range 3.729(4)–3.866(6) Å], and the average intracluster lead–oxygen distance 2.38(7) Å [range 2.22(5)–2.54(5) Å]. These hydroxide oxygen atoms are distributed in a distorted tetrahedron with the oxygen–oxygen distances in the range 2.60(7)–2.99(7) Å [av. 2.79(7) Å].

The nitrate groups occupy sites in the structure to balance the overall positive charge of the cluster cations. The nitrogen atoms are positioned 3.3–3.7 Å from the cluster atoms. For each nitrate group there are five to eight cluster atoms, the majority of which are lead atoms, closer than 4 Å. Apart from one nitrate group, which has only two nearest-neighbour clusters, the nitrates are surrounded by atoms from three separate clusters. The average nitrogen–oxygen bond length in the nitrate groups

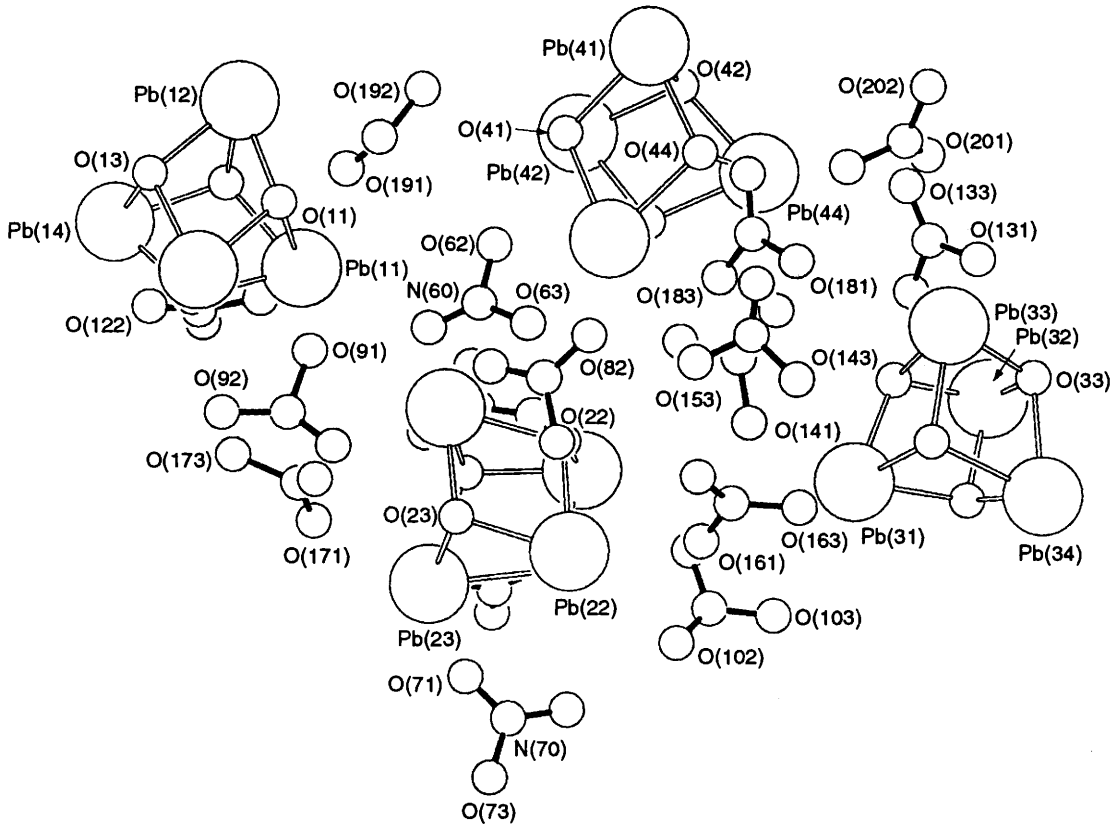

Fig. 2 Asymmetric unit of $[Pb_4(OH)_4][NO_3]_4$

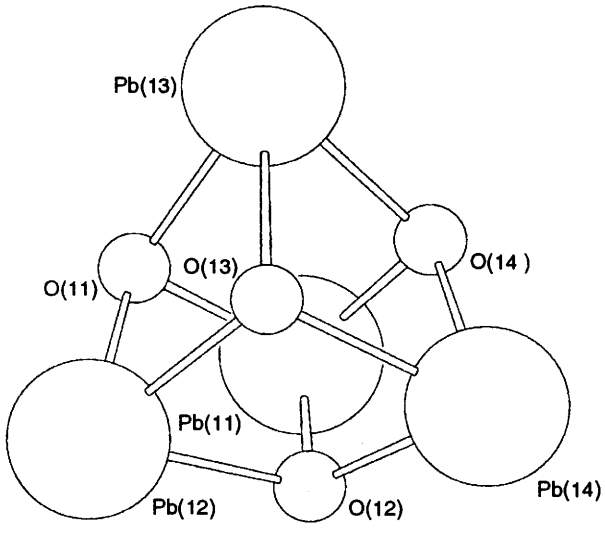

Fig. 3 Arrangement of atoms in a $[Pb_4(OH)_4]^{4+}$ cluster

is 1.24(9) Å and analysis of the bond angles shows that all the nitrate ions exhibit some degree of distortion. The average O–N–O bond angle is 119.6(8)°; range 105.0(7)–140(1)°. This distortion of the symmetry of the nitrate groups suggests a reasonable degree of interaction between the nitrate groups and the $[Pb_4(OH)_4]^{4+}$ clusters.

The $[Pb_4(OH)_4]^{4+}$ clusters are similar but not identical, with the range of distances for the four clusters being 3.73–3.82 for cluster 1 [Pb(11), Pb(12), Pb(13), Pb(14)], 3.74–3.87 for cluster 2 [Pb(21), Pb(22), Pb(23), Pb(24)], 3.75–3.84 for cluster 3 [Pb(31), Pb(32), Pb(33), Pb(34)] and 3.72–3.87 Å for cluster 4 [Pb(41), Pb(42), Pb(43), Pb(44)]. The average intracluster Pb–Pb–Pb bond angle is 60.0(1)° with the following ranges 58.6–61.2, 58.7–62.1, 59.0–61.7 and 58.5–61.5° for clusters 1, 2, 3 and 4 respectively. The four OH groups situated above the faces of the Pb_4 tetrahedra also form a distorted tetrahedral grouping in which the ranges of bond distances and angles (averages in parentheses) are: 2.59–2.82 (2.72) and 55.2–63.8 (60.0) for cluster 1, 2.62–2.82 (2.75) and 55.2–63.6 (60.0) for cluster 2, 2.78–2.99 (2.87) and 56.7–64.0 (60.0) for cluster 3, 2.75–2.92 (2.83 Å) and 57.4–63.8 (60.0°) for cluster 4.

The immediate environment of all of the lead atoms in $[Pb_4(OH)_4][NO_3]_4$ is a distorted trigonal-pyramidal arrangement of three nearest-neighbour cluster-hydroxide atoms. The average Pb–OH distance in the structure is 2.38(7) Å while the average Pb–OH distances in the individual clusters are 2.36, 2.37, 2.40 and 2.39 Å respectively. The Pb environments within each cluster do vary and the ranges of bond lengths are 2.22–2.47, 2.22–2.48, 2.27–2.54 and 2.31–2.45 Å respectively. The average OH–Pb–OH angle is 71.8(2)° and the ranges of cluster OH–Pb–OH bond angles (average in parentheses) for the four distinct clusters are 69.8–71.0 (70.3), 69.1–72.8 (70.8), 72.4–74.6 (73.5) and 71.1–73.3 (72.6)°. The next-nearest Pb–O distances are to nitrate O atoms with the shortest of these being in the range 2.62–2.80 Å. These longer Pb–O distances complete a distorted co-ordination of oxygen atoms around the lead in which the close approach of nitrate O atoms to the cluster Pb atoms is prevented by stereochemically active non-bonding electron pairs on the Pb atoms. Lead–oxygen distances of up to 3.25 Å have been taken as the maximum distance over which bonding interactions between Pb and O atoms could occur.[14] Applying this value to $[Pb_4(OH)_4][NO_3]_4$ the complete co-ordination of the lead atoms would be between nine and twelve. There is no doubt, however, that the most significant Pb–O bonding interactions are the short bonds to the cluster hydroxide groups and that any interactions with nitrate groups will be reduced by the position of the non-bonding electron pairs on the lead.

The closest distance between a lead atom and nitrate-oxygen

atoms (at 2.60–2.80 Å) is however considerably shorter than the minimum lead–perchlorate-oxygen distance of 2.96 Å previously reported for a basic lead(II) perchlorate.[14] These results clearly imply a significantly stronger degree of interaction between the lead and the nitrate oxygens than interactions reported for other related lead–hydroxo cluster compounds.[14,16]

Between neighbouring clusters the shortest Pb–Pb and Pb–OH interatomic distances are 4.126(6) and 3.91(5) Å respectively. Although these distances are considerably shorter than the values of 4.40 and 4.51 Å reported[14] for $[Pb_4(OH)_4]_3[CO_3][ClO_4]_{10}\cdot 6H_2O$, they are too long to imply any significant degree of interaction between clusters, indicating that they are best represented as discrete units. The minimum distance from a hydroxide-oxygen atom in the cluster to a nitrate oxygen was found to be 2.77(9) Å. Since hydrogen bonding has been considered to occur at O ··· O distances less than 3.15 Å,[22] the fact that two to six nitrate oxygen atoms lie close enough to each of the hydroxide groups, the $[Pb_4(OH)_4]^{4+}$ clusters, although discrete, may be held in the lattice by a hydrogen-bonding network.

Although the average lead–lead distance [3.785(4) Å] could arise from the constraints of the cluster, it is short enough to consider the possible presence of lead–lead bonding interactions. Since the non-bonding electron-pair orbitals on the lead atoms in the cluster must point outwards from the cluster they cannot be taking part in metal–metal cluster bonding interactions and for this reason the short cluster Pb–Pb distances must arise because of the geometric constraints of forming the cluster and not from metal–metal bonding. Similar effects have been observed in tin(II)–hydroxo clusters.[23]

The overall characteristics of the $[Pb_4(OH)_4]^{4+}$ cluster reported here correlate well with those obtained for this unit in the only related crystal structure,[14] $[Pb_4(OH)_4]_3[CO_3][ClO_4]_{10}\cdot 6H_2O$, and with the results obtained from X-ray scattering measurements in aqueous solution.[9] In the crystal structure of $[Pb_4(OH)_4]_3[CO_3][ClO_4]_{10}\cdot 6H_2O$, the average Pb–Pb and Pb–O distances were 3.76 and 2.80 Å, respectively. The X-ray scattering data of lead(II)–perchlorate solutions were interpreted in terms of an average Pb–Pb distance of 3.85 Å and two sets of average Pb–O distances of 2.4 and 2.9 Å, which we now confirm to be the expected average intra- and extra-cluster Pb–O distances from $[Pb_4(OH)_4][NO_3]_4$.

The Raman-active bands for $[Pb_4(OH)_4][NO_3]_4$ in the range 100–1634 cm^{-1} are in Table 3; those between 60 and 505 cm^{-1} have been assigned[12] to the $[Pb_4(OH)_4]^{4+}$ unit, and the bands at 133.8 and 404.9 cm^{-1} correspond well with previous values; the remaining bands in the range 100–700 cm^{-1} which were not observed in this study were noted as being weak or uncertain in prior work.[8] Above 700 cm^{-1} the spectrum is essentially that of a free nitrate ion.[24] There is splitting of the peak at 716.9 cm^{-1} giving a shoulder at 705.6 cm^{-1} arising from a reduction in the symmetry of the nitrate because of weak bonding interactions with the clusters. The presence of the nitrate band at 823.9 cm^{-1} which would be Raman inactive for an ion with D_{3h} symmetry is consistent with a reduction in the symmetry of the NO_3^- group because of nitrate–oxygen interactions with the $[Pb_4(OH)_4]^{4+}$ cluster.

The thermogravimetric (TG) and differential thermal analysis (DTA) data for $[Pb_4(OH)_4][NO_3]_4$ are in Table 4. These data correlate well with those previously reported[8,25] for $Pb(OH)_2\cdot Pb(NO_3)_2$ and are now interpreted in the light of the crystal structure. The first two steps in the decomposition process (weight loss endotherms at 95 and 130 °C) correspond to the loss of two water molecules resulting from the decomposition of the $[Pb_4(OH)_4]^{4+}$ unit in two stages, equation (1). The third step (endotherm at

$$[Pb_4(OH)_4]^{4+} \longrightarrow [Pb_4O(OH)_2]^{4+} + H_2O \longrightarrow [Pb_4O_2]^{4+} + H_2O \quad (1)$$

180 °C) is a phase transition confirmed by changes in the DTA curve and the absence of any corresponding weight loss on the TG curve. The remaining four steps (weight loss endotherms at 350, 390, 420 and 450 °C) correspond to the progressive decomposition of the nitrate groups in the sample. The route for the nitrate decomposition is outlined in Scheme 1. The theoretical weight losses for the proposed decomposition stages are compared to the observed data in Table 4.

Table 3 Raman spectral data (cm^{-1}) of $[Pb_4(OH)_4][NO_3]_4$

Observed data *	Calculated values [12]	Observed data for $PbO\cdot Pb(NO_3)_2\cdot 2H_2O$ [8]
		35
	60	60
	87	93
133.8(11)	130	132
	346	360
404.9(11)	404	403
	455	
	505	
716.9(7)		717
823.9(10)		
1045.1(100)		1049
1381.7(8)		1395
1633.8(4)		

* Relative intensity in parentheses.

Table 4 The thermal decomposition of $[Pb_4(OH)_4][NO_3]_4$

Step	Weight loss (%) *	Onset temperature/°C
1	1.60 (1.57)	95
2	1.60 (1.57)	130
3	0.00 (0.00)	180
4	3.20 (3.15)	350
5	3.20 (3.15)	390
6	6.30 (6.30)	420
7	6.30 (6.30)	450
Total	22.19 (22.04)	

* Calculated values in parentheses.

$$Pb_{12}O_6(NO_3)_{12}$$
$$\downarrow$$
$$Pb_{12}O_7(NO_3)_{10} + 2NO_2 + \tfrac{1}{2}O_2$$
$$\downarrow$$
$$Pb_{12}O_8(NO_3)_8 + 2NO_2 + \tfrac{1}{2}O_2$$
$$\downarrow$$
$$Pb_{12}O_{10}(NO_3)_4 + 4NO_2 + O_2$$
$$\downarrow$$
$$Pb_{12}O_{12} + 4NO_2 + O_2$$

Scheme 1

The first precipitate obtained when the pH of a lead nitrate solution is raised is confirmed as the distinct basic salt $[Pb_4(OH)_4][NO_3]_4$. In the pH titration curve (Fig. 1) this phase is shown to be precipitated in a narrow pH range around 5.3 as hydroxide ion is added to precipitate all of the lead as $[Pb_4(OH)_4][NO_3]_4$. After all of the lead is precipitated the pH rises to about 7.0 where again the addition of alkali solution results in the uptake of hydroxide ion rather than increase in pH. A second distinct crystalline phase is formed at pH 7.0 which has been previously formulated[6] as $2Pb(NO_3)_2\cdot 5Pb(OH)_2$, but which is more likely to be $[Pb_3(OH)_4][NO_3]_2$,

Table 5 Analytical data for products formed in the Pb^{2+}–OH^-–NO_3^- system

pH	Compound	Analyses (%)*		
		Pb^{2+}	OH^-	NO_3^-
5.25	$Pb_4(OH)_4(NO_3)_4$	72.0 (72.4)	6.05 (6.0)	21.7 (21.7)
7.03	$Pb_3(OH)_4(NO_3)_2$	76.1 (76.4)	8.8 (8.4)	14.5 (15.2)
8.5	$Pb_6O(OH)_6(NO_3)_4$	79.1 (81.8)	8.3 (9.0)	8.2 (8.2)

* Calculated values in parentheses.

similar to the distinct basic tin(II) salt[23] $[Sn_3(OH)_4][NO_3]_2$. The second distinct phase could be formed from $[Pb_4(OH)_4][NO_3]_4$ by the gradual replacement of nitrate ions in the lattice by hydroxide resulting in the collapse of the structure and the reformation of the new phase or by changes in the equilibrium in the small part of the material that is dissolved away from $[Pb_4(OH)_4]^{4+}$ towards $[Pb_3(OH)_4]^{2+}$ or similar species. When all of the lead is converted to the second distinct phase, addition of hydroxide results in an increase to pH 8.5 where a third distinct phase is formed. The analytical data in Table 5 suggest that this could be a derivative of the known $[Pb_6O(OH)_6]^{4+}$ ion. Again this third phase could result from hydroxide replacement of nitrate ions resulting in a lattice rearrangement or by movements in the dilute solution equilibria resulting in the formation of a Pb_6–hydroxo cluster which loses one molecule of water at the point of precipitation. Further additions of alkali solution result in an increase in the pH until at pH *ca.* 11.2 the final product, hydrous lead(II) oxide, is formed.

When metal species are leached from minerals or enter the aqueous systems from effluent, they do so at a pH that is approximately neutral and their transport in the environment must depend upon their chemical behaviour under those conditions. Assumptions are often made that the metals dissolve as hydrated cations, and are then precipitated as hydroxides. Such assumptions are not, however, always consistent with the chemistry of the metal-containing species present under the appropriate conditions and this can lead to errors in descriptions of their transport. Three major factors have to be taken into consideration in determining the nature of metal-containing species once they have entered the aqueous environment, *viz.*, the relative stabilities of the hydrated metal cations and precipitated hydroxide-containing phases in aqueous systems of appropriate pH; the formation of polymeric complex metal–hydroxo species and their precipitation as basic salts; and the presence of any anion or complexing groups that might lead to precipitation or formation of soluble metal complexes respectively. We have shown that in the case of lead three distinct lead–hydroxo species are formed in the pH range 5.25–8.5—a range that is typical of the natural aqueous environment. Any attempt therefore to study the interactions between hydroxide precipitates of lead and soil components and biological tissues must take into consideration the likely presence in solution of the cluster cations $[Pb_4(OH)_4]^{4+}$, $[Pb_3(OH)_4]^{2+}$ and $[Pb_6O(OH)_6]^{4+}$ and of precipitates containing them. Evidence suggests that although the precipitates obtained can be crystalline under suitable conditions reaction with hydroxide in aqueous systems usually leads to less crystalline materials of smaller particle size and higher surface activity. This increased activity will increase the ability of the lead-containing precipitates to adhere to and react with soil and biological components of ecosystems. The transport of lead in aqueous systems and soils and into biological systems must depend upon the properties of the soluble and precipitated lead hydroxide clusters described in this work and not on Pb^{2+} ions or simple hydroxides.

Acknowledgements

We thank the SERC for an award to S. R. J. We also thank M. Motevalli at Queen Mary and Westfield College, London for data collection and Professor D. N. Batchelder at Leeds University for use of a Raman imaging microscope.

References

1 H. Guiter, *Bull. Soc. Chim. Fr.*, 1947, 269.
2 A. Berton, *Bull. Soc. Chim. Fr.*, 1947, 289.
3 M. Geloso and J. Faucherre, *C. R. Acad. Sci.*, 1948, **227**, 1243.
4 J. Heubel, *Ann. Chim. (Paris)*, 1949, 701.
5 J. L. Pauley and M. K. Testerman, *J. Am. Chem. Soc.*, 1954, **76**, 4220.
6 W. Kwestroo, C. Langereis and H. A. M. van Hal, *J. Inorg. Nucl. Chem.*, 1967, **29**, 33.
7 E. Narita, H. Okayasu and H. Naito, *Bull. Chem. Soc. Jpn.*, 1984, **57**, 309.
8 A. G. Cram and M. B. Davies, *J. Inorg. Nucl. Chem.*, 1976, **38**, 1111.
9 A. Olin, *Acta. Chem. Scand., Ser. A*, 1960, **14**, 126.
10 A. Olin and G. Johansson, *Acta Chem. Scand., Ser. A*, 1968, **22**, 3197.
11 O. E. Esval, Ph. D. Thesis, University of North Carolina, 1962.
12 V. A. Marino and T. G. Spiro, *Inorg. Chem.*, 1968, **7**, 188.
13 V. A. Marino and T. G. Spiro, *J. Am. Chem. Soc.*, 1966, **89**, 45.
14 A. Olin and Sam-Hyo Hong, *Acta Chem. Scand., Ser. A*, 1973, **27**, 2309.
15 T. G. Spiro, D. H. Templeton and A. Zalkin, *Inorg. Chem.*, 1969, **8**, 856.
16 A. Olin and R. Sonderquist, *Acta Chem. Scand., Ser. A*, 1972, **26**, 3505.
17 A. I. Vogel, *Textbook of Quantitative Chemical Analysis*, Longman Scientific and Technical, London, 5th edn., 1989.
18 K. P. J. Williams, G. D. Pitt, D. N. Batchelder and B. J. Kip, *Appl. Spectrosc.*, 1994, **48**, 232.
19 G. M. Sheldrick, SHELXS 86, Program for Crystal Structure Solution, University of Göttingen, 1986.
20 G. M. Sheldrick, SHELX 76, Program for Crystal Structure Determinations, University of Cambridge, 1976.
21 G. M. Sheldrick, SHELXL 93, Program for Crystal Structure Refinement, University of Göttingen, 1993.
22 *International Tables for X-Ray Crystallography*, Kynoch Press, Birmingham, 1974, vol. 3.
23 J. D. Donaldson, S. M. Grimes, S. R. Johnston and I. Abrahams, *J. Chem. Soc., Dalton Trans.*, in the press.
24 S. D. Ross, *Inorganic Infrared and Raman Spectra*, McGraw-Hill, London, 1972.
25 M. E. Garcia-Clavel, M. J. Martinez-Lope, M. T. Casias-Alvarez and A. Kilany, *Thermochim. Acta*, 1986, **98**, 205.

Received 9th December 1994; *Paper* 4/07524B